Research Square

Preprints are preliminary reports that have not undergone peer review.
They should not be considered conclusive, used to inform clinical practice,
or referenced by the media as validated information.

Copper-Potentiated Disulfiram Cytotoxicity in HCT116 and SW480 Colorectal Cancer Cells: Redox Imbalance and Telomerase Suppression Without Direct Enzyme Inhibition

Mehdi Khorrami
Golestan University of Medical Sciences
Jahanbakhsh Asadi
Golestan University of Medical Sciences
Mohsen Tatar
mohsentatar@ymail.com

Golestan University of Medical Sciences

Research Article

Keywords: Colorectal cancer, Disulfiram, Copper, Telomerase, Glutathione, Oxidative stress

Posted Date: November 11th, 2026

DOI: https://doi.org/10.21203/rs.3.rs-10899395/v1

License: This work is licensed under a Creative Commons Attribution 4.0 International License.
Read Full License

Additional Declarations: No competing interests reported.

Copper-Potentiated Disulfiram Cytotoxicity in HCT116 and SW480 Colorectal Cancer Cells: Redox Imbalance and Telomerase Suppression Without Direct Enzyme Inhibition

Mehdi Khorrami[1], Jahanbakhsh Asadi[1], Mohsen Tatar[1,*]

[1] Metabolic Disorders Research Center, Golestan University of Medical Sciences, Gorgan, Iran

*Corresponding author: Mohsen Tatar, PhD, Assistant Professor of Clinical Biochemistry, Metabolic Disorders Research Center, Golestan University of Medical Sciences, Hirkan Boulevard, Central Organization, Gorgan 4918936316, Golestan Province, Iran. Email: mohsentatar@ymail.com

ORCID: 0000-0003-1937-4179

Abstract

Background: Disulfiram (DSF) is being repurposed as a copper-dependent anticancer agent, but whether its activity involves telomerase, and by what route, remains undefined.

Methods: HCT116 and SW480 colorectal cancer cells were exposed for 48 h to copper sulfate, DSF, or DSF plus 0.1 μM copper, and viability was measured by MTT. Telomerase activity (telomeric repeat amplification protocol), reduced glutathione (GSH), and reactive oxygen species (ROS) were assessed after 24 h in intact cells, and telomerase was also assayed in cell-free lysates, over six independent biological replicates.

Results: DSF IC_{50} values were 2.04 μM (HCT116) and 1.73 μM (SW480); 0.1 μM copper reduced them to 0.39 and 0.56 μM. DSF lowered telomerase activity in HCT116 ($P < 0.005$), and DSF/copper lowered it in both lines ($P < 0.001$) while depleting GSH and raising ROS. In cell-free lysates, copper-containing conditions instead increased telomerase activity slightly ($P < 0.05$). GSH correlated with telomerase activity ($\rho = 0.75$) and inversely with ROS ($\rho = -0.85$), and ROS inversely with telomerase activity ($\rho = -0.80$).

Conclusions: Sub-toxic copper potentiates DSF cytotoxicity alongside redox imbalance and telomerase suppression. The opposite cell-free response argues against direct enzyme inhibition and supports an indirect, redox-linked mechanism.

Keywords: Colorectal cancer; Disulfiram; Copper; Telomerase; Glutathione; Oxidative stress

Abbreviations

ALDH, aldehyde dehydrogenase; BSA, bovine serum albumin; CuET, bis-diethyldithiocarbamate-copper; DCF, 2′,7′-dichlorofluorescein; DSF, disulfiram; DTNB, 5,5′-dithiobis(2-nitrobenzoic acid); DTT, dithiothreitol; FBS, fetal bovine serum; GSH, reduced glutathione; GSSG, oxidized glutathione; GSR, glutathione reductase; H_2DCFDA, 2′,7′-dichlorodihydrofluorescein diacetate; IC_{50}, half-maximal inhibitory concentration; KPE, potassium phosphate–EDTA buffer; MTT, 3-(4,5-dimethylthiazol-2-yl)-2,5-diphenyltetrazolium bromide; NAC, N-acetylcysteine; PAGE, polyacrylamide gel electrophoresis; PMSF, phenylmethylsulfonyl fluoride; RFU, relative fluorescence units; ROS, reactive oxygen species; SOD1, copper/zinc superoxide dismutase; TRAP, telomeric repeat amplification protocol.

1. Introduction

Colorectal cancer remains one of the principal contributors to the global cancer burden, with an estimated 1.93 million new cases and 0.90 million deaths worldwide in 2022, placing it third in incidence and second in cancer mortality [1]. The burden is not static. Incidence among adults under 50 years has risen steadily over the past three decades and is projected to continue climbing through the coming decade even as age-standardized mortality falls, a divergence that points to changing exposures rather than to improved detection alone [2]. Comparable trends are evident at the regional level: in Golestan province in northeastern Iran, population-based

registry data recorded a significant rise in colorectal cancer incidence between 2004 and 2018, with a consistent increase in risk across successive birth cohorts [3]. Against this background, and given the cost, duration, and high attrition of de novo drug development, there is a strong practical argument for revisiting agents whose pharmacology and safety are already established. Drug repurposing does precisely this, transferring existing knowledge to new indications and shortening the path to clinical evaluation [4].

Disulfiram (DSF), an inexpensive drug licensed for the treatment of alcohol dependence since the 1950s, has become one of the most intensively studied repurposing candidates in oncology [5]. Its anticancer activity is conditional rather than intrinsic: it requires copper. An early demonstration of this principle showed that the DSF–copper complex inhibits proteasomal activity and induces apoptosis selectively in breast cancer cells and xenografts, while sparing non-transformed cells, and that breast cancer cells containing physiological concentrations of copper undergo proteasome inhibition when exposed to DSF alone [6]. The molecular target was subsequently resolved. In cells exposed to copper, the DSF metabolite diethyldithiocarbamate forms bis(diethyldithiocarbamate)-copper (CuET), which binds the NPL4 adaptor and disables the p97–NPL4 segregase, causing accumulation of ubiquitinated proteins and severe proteotoxic stress [7]; targeted genetic and biochemical work later established that NPL4 engagement, rather than the inhibition of aldehyde dehydrogenase originally proposed, accounts for the principal anticancer activity of the drug [8].

Copper itself has meanwhile been reframed. It is now recognized to trigger a distinct, mitochondrially dependent form of regulated cell death, termed cuproptosis, in which copper binds lipoylated components of the tricarboxylic acid cycle and provokes lipoylated-protein aggregation, loss of iron–sulfur cluster proteins, and proteotoxic stress [9]. Because copper homeostasis is frequently disturbed in tumors, and because both copper excess and copper deprivation can be exploited therapeutically, deliberate manipulation of intracellular copper

has become an active therapeutic strategy in its own right [10]. Copper in the DSF–copper pair is therefore not a passive cofactor but a cytotoxic effector, which makes this combination mechanistically distinctive among repurposed agents and, at the same time, harder to attribute to a single target.

Evidence specific to colorectal cancer has accumulated rapidly and now spans several distinct mechanisms. The DSF–copper complex reduces colorectal cancer cell viability and induces ULK1-dependent autophagic cell death [11], and DSF has more recently been shown to activate autophagy in colorectal cancer cells through two convergent routes, compensatory induction downstream of p97–NPL4-mediated proteasome inhibition and transcriptional upregulation of BECN1 through c-Fos, with the addition of an autophagy inhibitor producing synergistic antitumor efficacy *in vitro* and *in vivo* [12]. The effects extend beyond the tumor cell itself: CuET remodels the colorectal tumor microenvironment, increasing lymphocyte infiltration and natural killer and T-cell cytotoxicity through the NKG2D–NKG2DL axis and converting immunologically cold tumors into responsive ones [13]. Clinical translation, however, has lagged behind this mechanistic progress. In a phase 1/2 study combining DSF and copper with radiotherapy and temozolomide in newly diagnosed glioblastoma, CuET was measurable in plasma but could not be detected in tumor tissue, and benefit was confined to a small BRAF-mutant subgroup [14]. Establishing which intracellular processes are actually engaged, and by what route, is therefore not merely of mechanistic interest but is central to deciding how this combination should be developed.

Two candidate processes converge on cellular redox state. Reduced glutathione (GSH) is the principal intracellular thiol antioxidant and a major determinant of redox homeostasis and treatment resistance in cancer [15], and in melanoma cells DSF-induced apoptosis is accompanied by oxidative stress and disruption of the glutathione redox system [16]. Telomerase, reactivated in the great majority of human cancers, sustains the replicative

capacity on which malignant cells depend [17]. Critically for the present question, telomerase in colorectal cancer has recently been shown to be under direct metal-ion control: working in fresh surgical specimens, Shanmugam and colleagues identified the iron sensor Pirin as a factor that reactivates the dormant human telomerase reverse transcriptase (hTERT) subunit in an Fe(III)-dependent manner, and showed that a small molecule competing with iron binding blocks this reactivation [18]. This provides the first mechanistic account of how a metal ion can reactivate telomerase and drive colorectal carcinogenesis, and it makes the behaviour of telomerase in the presence of an added transition metal a question worth asking directly. Telomerase and redox state are also reciprocally coupled in this tumor type; in HCT116 cells, knockdown of TERT or of the telomerase RNA component raises hydrogen peroxide levels and shifts the metabolic profile towards oxidative stress [19]. In the opposite direction, experimental GSH depletion lowers telomerase activity in fibroblasts and GSH repletion restores it [20], and in pancreatic cancer cells the triterpenoid CDDO-Me suppresses hTERT expression and telomerase activity through a reactive oxygen species (ROS)-dependent mechanism that antioxidants reverse [21].

These strands have not previously been brought together in a single experimental system. It remains unknown whether the copper-dependent cytotoxicity of DSF in colorectal cancer is accompanied by coordinated changes in glutathione, ROS, and telomerase activity and, if it is, whether telomerase is inhibited by the drug itself or by the redox environment that the drug creates. The distinction is not semantic. A direct effect would identify telomerase as a druggable target of DSF/copper; an indirect one would place telomerase downstream of redox stress and would predict that antioxidant rescue, rather than telomerase-directed strategies, is the appropriate test of causality. Given that a metal ion is now known to act positively on telomerase in this very tumor type [18], neither outcome can be assumed in advance. Accordingly, the present study quantified viability after DSF with or without a fixed sub-toxic

copper concentration in HCT116 and SW480 cells, measured telomerase activity in parallel intact-cell and cell-free assays designed specifically to separate direct from indirect action, assessed reduced glutathione and intracellular ROS under sub-lethal conditions, and examined the associations among these endpoints across both cell lines.

2. Materials and Methods

2.1 Reagents and instrumentation

Disulfiram (cat. no. A10320; CAS 97-77-8; ≥99% by HPLC) was obtained from Adooq Bioscience (Irvine, CA, USA) and dissolved in dimethyl sulfoxide (molecular-biology grade, cat. no. D8418; Sigma-Aldrich, Merck KGaA, Darmstadt, Germany) as a concentrated stock stored at −20 °C protected from light; the final solvent concentration in culture never exceeded 0.1% (v/v) and vehicle-matched controls were included throughout. Copper(II) sulfate pentahydrate was of analytical grade and prepared fresh in sterile deionized water. MTT and bovine serum albumin were from Solarbio Life Sciences (Beijing, China). 5,5′-Dithiobis(2-nitrobenzoic acid) (DTNB), 5-sulfosalicylic acid, Triton X-100, and potassium phosphate salts were from Merck (Darmstadt, Germany); glycerol, EGTA, and 2′,7′-dichlorodihydrofluorescein diacetate (H_2DCFDA) were from Sigma-Aldrich (Merck KGaA, Darmstadt, Germany); phenylmethylsulfonyl fluoride (PMSF) was from Bio Basic (Markham, ON, Canada). RPMI-1640 medium was from Gibco (Thermo Fisher Scientific, Waltham, MA, USA), trypsin–EDTA from Ide Zist Notarkib (Tehran, Iran), fetal bovine serum from Biosera (Cholet, France), and phosphate-buffered saline from Dena Zist Asia (Mashhad, Iran). Taq DNA polymerase, dNTP mix, and $MgCl_2$ were from Pars Tous Biotechnology (Mashhad, Iran); 10× PCR buffer and Tris base from SinaClon BioScience (Tehran, Iran); TRAP primers were custom-synthesized by Pishgam Biotech (Tehran, Iran); and the GelRed-containing 5× PowerLoad pre-mixed nucleic-acid stain was from Kowsar Biotech (Tehran, Iran). Cell-culture

plasticware was from SPL Life Sciences (Pocheon, South Korea) and Jet Biofil (Guangzhou, China).

Absorbance readings were taken on a ChroMate microplate reader (Awareness Technology, Palm City, FL, USA); PCR was performed on an Applied Biosystems thermal cycler (Thermo Fisher Scientific, Waltham, MA, USA); electrophoresis used a Syngene system (Cambridge, UK) with imaging on a UVITEC gel documentation system (UVITEC Cambridge, Cambridge, UK); and lysates were clarified in a refrigerated centrifuge (Behdad, Tehran, Iran). Fluorescence was read on a fluorescence microplate reader.

2.2 Cell lines and culture conditions

The established human colorectal cancer cell lines HCT116 (RRID:CVCL_0291) and SW480 (RRID:CVCL_0546) were obtained from the National Cell Bank of Iran, Pasteur Institute of Iran (Tehran, Iran), and used within a limited number of passages after thawing. Experiments were performed at the Metabolic Disorders Research Center, Golestan University of Medical Sciences, with collaboration from Shiraz University of Medical Sciences. Cells were maintained as monolayers in RPMI-1640 supplemented with 10% (v/v) fetal bovine serum and 1% (v/v) penicillin–streptomycin at 37 °C, >90% relative humidity, and 5% CO_2, with medium renewed three times weekly. At approximately 70% confluence, cells were detached with trypsin–EDTA, centrifuged, and counted on a Neubauer hemocytometer. For all plate-based assays, 10,000 cells were seeded per well of a 96-well plate and allowed to attach for 24 h before treatment. The available study records did not specify exact passage ranges, STR-authentication dates, or mycoplasma-testing dates; these details were therefore not inferred and are acknowledged as a limitation.

2.3 Drug treatments and MTT viability assay

For dose–response experiments, cells were exposed for 48 h to 0.1–20 μM copper sulfate, 0.1–20 μM DSF, or DSF combined with a fixed sub-toxic copper concentration (0.1 μM). A separate DSF arm was tested in serum-free medium to assess the contribution of trace copper associated with serum. After treatment, the medium was replaced with 200 μL fresh medium containing 0.5 mg/mL MTT and the plates were incubated for 4 h at 37 °C. Formazan crystals were dissolved in dimethyl sulfoxide, absorbance was read at 570 nm, and viability was expressed relative to the vehicle-matched control. IC_{50} values were estimated from the dose–response curves in GraphPad Prism.

For the 24-h biochemical assays (telomerase activity, GSH, and ROS), both cell lines received a single fixed working concentration of 0.5 μM DSF alone, 0.1 μM copper sulfate alone, or 0.5 μM DSF plus 0.1 μM copper. This concentration lies close to the IC_{50} of the DSF/copper combination determined above (0.39 μM in HCT116 and 0.56 μM in SW480) and was deliberately kept below the IC_{50} of DSF alone, so that the biochemical endpoints were measured under sub-lethal conditions in which viable cells predominated and the readouts were not confounded by widespread cell death.

The two exposure times were chosen deliberately. Viability was assessed at 48 h, the interval over which the cytotoxic effect becomes fully established and a stable IC_{50} can be derived. The biochemical endpoints were assessed at 24 h because they are intended to capture the mechanistic events that precede cell death rather than its consequences. Once appreciable cell loss has occurred, GSH and ROS readouts increasingly reflect dying and detaching cells, and normalization to total protein becomes unreliable. Measuring these indices at 24 h, under sub-lethal conditions, therefore positions the observed redox and telomerase changes as upstream events rather than as secondary markers of cytotoxicity.

2.4 Protein extraction and quantification

After 24 h of treatment, cells were detached with trypsin, pelleted, and washed with ice-cold PBS. Pellets were lysed in 300 µL buffer containing 10 mM Tris-HCl (pH 7.5), 1 mM EGTA, 150 mM NaCl, 10% (v/v) glycerol, and 1% (v/v) NP-40, supplemented immediately before use with 0.1 mM PMSF and 5 mM dithiothreitol. Lysates were held on ice for 20 min and clarified by refrigerated centrifugation, and the supernatant containing soluble protein was collected. All steps were performed on ice to limit proteolysis.

Protein concentration was determined by the Bradford method [22] using bovine serum albumin standards: 30 µL lysate was mixed with 1480 µL Bradford reagent, incubated for 15 min at room temperature, and read at 595 nm.

2.5 Telomeric repeat amplification protocol (TRAP) assay

Telomerase activity was measured semi-quantitatively by TRAP, following the protocol previously applied to colorectal cancer cell lysates by this group [23]. For intact-cell experiments, 2 µg of cellular protein was incubated with the TS substrate primer and the primary reaction components for 30 min at 30 °C to allow telomerase-mediated primer extension. The ACX reverse primer together with the NT and TSNT internal-control primers, dNTPs, $MgCl_2$, and Taq DNA polymerase were then added, and the products were amplified over 35 PCR cycles. Primer sequences are given in Table 1.

Amplification products were mixed 5:1 with 5× PowerLoad pre-mixed stain, which incorporates the GelRed fluorescent dye directly during loading and eliminates the silver-staining and ethidium-bromide steps. Samples were resolved on a 12.5% non-denaturing polyacrylamide gel in 1× TBE at constant voltage, and the gel was transferred directly to the gel documentation system without any secondary staining or washing step. Telomeric ladders were visualized under ultraviolet illumination and quantified densitometrically in ImageJ.

Samples showing a laddering pattern were scored positive; samples showing only the 36-bp internal control band were scored negative. The 36-bp internal amplification control was used to exclude false negatives and to monitor amplification efficiency, and relative telomerase activity in each treatment group was expressed as a percentage of the vehicle-matched control (defined as 100%).

For the cell-free experiment, 2 μg of protein from untreated HCT116 lysate was incubated for 1 h at 37 °C with DSF (0.5 or 1 μM), copper sulfate (0.1 μM), or 1 μM DSF combined with 0.1 μM copper, before TRAP analysis under identical conditions. This design tested whether DSF or copper acts directly on the telomerase holoenzyme, independently of intracellular signaling.

2.6 Reduced glutathione assay

Intracellular GSH was measured spectrophotometrically with Ellman's reagent (DTNB), using an acidic deproteinizing extraction adapted from Rahman et al. [24]. A conventional Tris/NP-40 lysis buffer is unsuitable for this assay because free protein thiols also react with DTNB and inflate the apparent GSH concentration; acid extraction simultaneously precipitates protein and arrests glutathione-degrading enzyme activity.

KPE buffer was prepared as 100 mM potassium phosphate containing 1–2 mM EDTA (pH 7.5), and the extraction buffer, made fresh immediately before use, consisted of 0.1% (v/v) Triton X-100 and 0.6% (w/v) sulfosalicylic acid in KPE. After 24 h of treatment, cells were washed twice with ice-cold PBS, harvested by scraping, and centrifuged (approximately 3,000 rpm, 4 °C, 5 min). The pellet was resuspended in 100–200 μL extraction buffer, subjected to one freeze–thaw cycle (−70 °C followed by thawing on ice) to complete lysis and protein precipitation, and centrifuged at 4 °C to obtain a clear, protein-free supernatant. Because the supernatant is acidic, it was diluted in phosphate reaction buffer (pH 8.0) before reaction with

DTNB so that the final pH remained in the alkaline range required for color development. Absorbance was read at 412 nm within 5 min of DTNB addition, since longer intervals drive the reaction out of the linear range. GSH was quantified against a standard curve constructed from serial dilutions of a 1 mM GSH stock (0–100 µM), prepared at least in duplicate; the detection limit of the method was 0.3 µM. A separate aliquot of lysate taken before acidification was used for Bradford protein determination, and results were expressed as µM GSH per mg total protein.

2.7 Intracellular reactive oxygen species assay

Intracellular ROS were measured with the cell-permeant fluorogenic probe H_2DCFDA, which is hydrolyzed by intracellular esterases to non-fluorescent DCFH and oxidized by ROS to fluorescent 2′,7′-dichlorofluorescein; the assay followed the general microplate procedure of Wang and Joseph [25]. Cells were seeded at 10,000 cells per well in black-walled, clear-bottom 96-well plates to prevent light scatter and cross-well fluorescence bleed. Before treatment, the medium was replaced with phenol red-free medium, since phenol red produces background fluorescence in this wavelength range. After 24 h of treatment, cells were washed once with assay buffer and incubated with freshly prepared H_2DCFDA (10–20 µM final concentration) for 30–45 min at 37 °C in a CO_2 incubator in complete darkness, then washed again to remove unbound probe. Fluorescence was read immediately at 485 nm excitation and 528 nm emission and expressed as relative fluorescence units (RFU). Unstained blank wells were included for background subtraction, and a short hydrogen peroxide exposure served as a positive control to confirm probe performance and linearity. Working solutions of H_2DCFDA and DTNB were kept wrapped in aluminium foil throughout, reagents were dispensed rapidly and uniformly to equalize incubation times across wells, and bubble formation in the wells was avoided.

2.8 Statistical analysis

All assays were performed in six independent biological replicates, that is, six separate experiments each initiated from an independent cell culture. Within every biological replicate each sample was read in technical duplicate, and the mean of the two readings was taken as the value for that replicate; six independent values per treatment group per cell line therefore entered the statistical analysis (n = 6). The cell-free telomerase experiment was likewise performed in three independent runs (n = 3).

Data are presented as mean ± standard deviation. Group comparisons were made by one-way analysis of variance followed by Tukey's multiple-comparison test. Distributional assumptions were examined with the Shapiro–Wilk test. Because the pooled biochemical-index data were not normally distributed, associations among telomerase activity, GSH, and ROS were assessed with the non-parametric Spearman rank correlation across the four treatment groups in both cell lines, giving 48 values per index (two cell lines × four groups × six biological replicates). The Spearman coefficient (ρ) ranges from −1 to +1, with values near +1 indicating a strong positive monotonic relationship, values near −1 a strong negative relationship, and values near zero the absence of a monotonic relationship. Analyses were performed in GraphPad Prism and SPSS, and $P < 0.05$ was considered statistically significant.

2.9 Ethical considerations

This *in vitro* study used commercially established human colorectal cancer cell lines and involved no human participants, no animals, and no identifiable human biological material. The protocol was reviewed and approved by the Ethics Committee of Golestan University of Medical Sciences (approval code IR.GOUMS.REC.1403.113), and institutional biosafety procedures for the handling of chemical reagents and the disposal of biological waste were followed throughout.

3. Results

3.1 Copper potentiates disulfiram-induced growth inhibition in colorectal cancer cells

In HCT116 cells (Fig. 1), DSF in serum-free medium reduced viability from 100% at zero concentration to 64% at 20 μM, with the steepest decline occurring between 2 and 4 μM. In the presence of serum, DSF produced a markedly steeper decline, reaching 18.1% viability at 20 μM. When DSF was combined with a fixed copper concentration (0.1 μM) in the presence of serum, the decline was considerably sharper still, with mean viability reaching zero from 2 μM onward, indicating pronounced potentiation of DSF cytotoxicity by copper. In contrast, copper alone (with serum) left viability between 84% and 104% across the entire concentration range, showing that copper by itself has negligible effect on HCT116 viability while markedly potentiating DSF cytotoxicity when the two are combined.

The pattern in SW480 cells (Fig. 2) paralleled that seen in HCT116, although the magnitude of the decline differed in some groups. With serum, DSF reduced viability to 12% at 20 μM, a steeper decline than the corresponding value in HCT116 (18.1%). As in HCT116, the DSF–copper combination reduced mean viability to zero from 2 μM onward, while copper alone again left viability between 87% and 104% with no significant change. Overall, these results indicate that in both cell lines the growth-inhibitory effect of DSF is markedly potentiated by copper.

To quantify this potentiation, IC_{50} values were calculated from the dose–response curves (Table 2). DSF alone (with serum) yielded IC_{50} values of 2.04 μM in HCT116 and 1.73 μM in SW480. Addition of 0.1 μM copper reduced these values to 0.39 μM in HCT116 and 0.56 μM in SW480, corresponding to approximately 5.3-fold and 3.1-fold potentiation of cytotoxicity, respectively. Because copper alone and DSF under serum-free conditions did not produce

sufficient loss of viability within the tested concentration range (up to 20 μM), IC_{50} could not be calculated for these groups.

3.2 Effect of disulfiram and copper on telomerase activity in intact cells

In HCT116 cells, telomerase activity decreased in a treatment-dependent manner (Fig. 3; Table 3). Baseline activity in the control group was 101.5 ± 2.25%. DSF alone significantly reduced this activity to 86.8 ± 4.26% ($P < 0.005$). Co-treatment with copper intensified the reduction, lowering telomerase activity to the lowest level observed among all groups, 69.4 ± 8.22% ($P < 0.001$). Copper alone had no significant effect, remaining close to baseline at 98.4 ± 1.56%.

A similar but less pronounced pattern was observed in SW480 cells (Fig. 3; Table 3). Baseline telomerase activity in the control group was 100.9 ± 2.55%. DSF alone produced only a modest, statistically non-significant reduction, to 95.0 ± 5.39%. The DSF–copper combination, however, produced a significant reduction to 78.6 ± 6.97% ($P < 0.001$). As in HCT116, copper alone produced no significant change relative to control (99.5 ± 3.50%). Taken together, DSF alone was sufficient to inhibit telomerase activity significantly in HCT116 cells, whereas the concurrent presence of copper substantially potentiated this inhibitory effect in both cell lines, and copper sulfate alone lacked any appreciable inhibitory effect.

Representative TRAP gels for both cell lines are shown in Fig. 3A. In each cell line, the telomeric ladder generated in the DSF plus copper lane was visibly attenuated, in both band number and band intensity, relative to the untreated control lane, whereas the copper-only lane was indistinguishable from control. The 36-bp internal amplification control was detected in every sample lane, indicating comparable amplification efficiency across conditions and excluding false-negative results.

3.3 Effect of disulfiram and copper on telomerase activity in a cell-free system

Having observed the anti-telomerase effect of DSF in intact cells, we next examined whether DSF and copper act directly on the telomerase enzyme in a cell-free system. Untreated HCT116 lysate (2 μg protein) was incubated for 1 h at 37 °C with DSF (0.5 or 1 μM), copper (0.1 μM), or 1 μM DSF combined with 0.1 μM copper (Fig. 4).

Incubation with 0.1 μM copper produced a significant increase in telomerase activity of 7.6 ± 4.4% relative to control ($P < 0.05$). DSF alone, at either concentration, produced no significant change. The DSF–copper combination produced a significant increase of 8.7 ± 3.9% relative to control ($P < 0.05$). Consistent with this, telomeric ladders were retained in all lanes of the representative gel (Fig. 4A), with no loss of banding in the DSF-containing conditions.

These findings indicate that the modest stimulation observed in the copper-containing groups of the cell-free system is attributable to the copper ion itself, independent of cellular context. Critically, they also show that the inhibition seen in intact cells is not the result of a direct action of DSF on the telomerase holoenzyme, but instead depends on intracellular mechanisms.

3.4 Effect of disulfiram and copper on reduced glutathione levels

In HCT116 cells (Fig. 5; Table 3), the baseline GSH concentration in the control group was 22.30 ± 0.60 μM/mg protein. Copper alone produced no significant change (21.40 ± 0.70 μM/mg protein; $P = 0.36$). DSF alone significantly reduced GSH to 18.86 ± 1.64 μM/mg protein ($P < 0.05$), and the DSF–copper combination intensified this reduction further, lowering GSH to the lowest level among all groups, 14.94 ± 1.27 μM/mg protein ($P < 0.001$ versus control).

Similar results were obtained in SW480 cells (Fig. 5; Table 3). The baseline GSH concentration in the control group was 24.60 ± 1.00 μM/mg protein, and copper alone produced no significant change (23.90 ± 0.90 μM/mg protein; $P = 0.81$). DSF alone significantly reduced GSH to 22.64

± 1.78 μM/mg protein ($P < 0.05$), and the DSF–copper combination further intensified this reduction, lowering GSH to 18.75 ± 1.27 μM/mg protein ($P < 0.05$ versus control). Taken together, copper alone had no appreciable effect on cellular GSH reserves, whereas DSF alone significantly depleted GSH in both cell lines, an effect markedly potentiated by copper.

3.5 Effect of disulfiram and copper on intracellular ROS levels

In HCT116 cells (Fig. 6; Table 3), baseline ROS in the control group was 116.6 ± 5.2 RFU. Copper sulfate alone produced no significant change (121.3 ± 6.0 RFU; $P = 0.99$). DSF alone markedly increased ROS to 158.3 ± 10.4 RFU ($P < 0.001$), and co-administration of copper further intensified this increase, reaching the highest ROS level among all groups examined, 193.1 ± 17.8 RFU ($P < 0.001$ versus control).

A similar trend was observed in SW480 cells (Fig. 6; Table 3). Baseline ROS in the control group was 102.2 ± 6.8 RFU, and copper alone produced no significant change (105.0 ± 2.9 RFU; $P = 0.87$). DSF alone significantly increased ROS to 135.4 ± 5.1 RFU ($P < 0.001$), and the DSF–copper combination intensified this increase further, raising ROS to 156.4 ± 9.1 RFU ($P < 0.001$ versus control). These findings indicate that copper alone has no appreciable effect on baseline intracellular ROS, whereas DSF alone significantly increases ROS production in both cell lines, an effect markedly potentiated by copper and mirroring the parallel, copper-dependent depletion of cellular GSH reserves described above.

3.6 Correlation between telomerase activity, GSH, and ROS

Because the pooled data for each index were not normally distributed by the Shapiro–Wilk test, relationships among the variables were assessed using the non-parametric Spearman correlation. The results, summarized in Table 4, revealed statistically significant relationships among all three indices.

The correlation between GSH concentration and telomerase activity was strongly positive ($\rho = 0.75$, $P < 0.001$), indicating that as GSH levels declined across the treatment groups, telomerase activity declined concomitantly. A strong negative correlation was observed between GSH concentration and ROS level ($\rho = -0.85$, $P < 0.001$), indicating that depletion of the cellular antioxidant reserve was accompanied by a significant rise in ROS. Likewise, a strong negative correlation was found between ROS level and telomerase activity ($\rho = -0.80$, $P < 0.001$), indicating that increased oxidative stress was accompanied by reduced telomerase activity.

This triangular pattern of associations offers a coherent picture of the sequence of events that may underlie the effect of the DSF–copper combination: depletion of reduced glutathione, disruption of redox balance with a rise in reactive oxygen species, and consequent suppression of telomerase catalytic activity. The pattern is fully consistent with the preceding sections, in which the inhibitory effect of DSF on telomerase was observed in intact cells but not in the cell-free system.

4. Discussion

This study evaluated DSF alone and in combination with copper in HCT116 and SW480 colorectal cancer cells. Beyond viability and IC_{50}, telomerase activity, GSH, and ROS were measured, and their associations were explored. The data show copper-dependent potentiation of DSF cytotoxicity accompanied by redox imbalance and reduced telomerase activity in intact cells. Because the same treatments did not inhibit telomerase in cell-free lysates, the findings point towards an indirect, cellular-context-dependent mechanism rather than direct enzyme inhibition; they do not, by themselves, establish a causal pathway.

4.1 Copper potentiation of disulfiram cytotoxicity

DSF alone showed moderate antiproliferative activity, with IC_{50} values of 2.04 μM in HCT116 and 1.73 μM in SW480. Adding 0.1 μM copper reduced these values to 0.39 and 0.56 μM, corresponding to 5.3- and 3.1-fold potentiation, respectively. Because no combination-index or isobologram analysis was performed, these data support potentiation rather than formal pharmacological synergy. The pattern is compatible with the formation of CuET and disruption of the NPL4–p97 pathway [7,8], which can produce replication stress and proteostasis failure [26] as well as translational arrest, p53 aggregation, and ribosome-biogenesis stress [27]. It is worth noting that the copper contributed by the combination is not necessarily inert once CuET has formed. Copper excess is itself capable of triggering cuproptosis through the aggregation of lipoylated tricarboxylic acid cycle proteins and the consequent loss of iron-sulfur cluster proteins [9], and disturbed copper homeostasis is increasingly regarded as a therapeutic vulnerability in its own right [10]. At the 0.1 μM concentration used here, however, copper alone was demonstrably non-cytotoxic across the full range tested, so cuproptosis is unlikely to account for the effects reported below. The point is rather that copper occupies a dual position in this system, as the activator of the drug and as a potential effector, and the two contributions cannot be separated by viability data alone.

Neither copper alone nor DSF in serum-free medium reached an IC_{50} within the tested range. This supports, but does not prove, a requirement for available copper in DSF activation [5]. The cytotoxic activity of DSF is exerted largely through CuET rather than through the parent molecule, so that in the absence of sufficient environmental copper the active complex cannot form in adequate quantity and DSF remains as the parent compound or as unstable, weakly active metabolites.

Quantitative comparison with earlier reports is informative. Yip and colleagues showed in several breast cancer cell lines that DSF becomes appreciably cytotoxic only in the presence of

1 μM extracellular copper, with IC_{50} values in the 200–500 nM range, and attributed this to ROS generation, activation of JNK and p38 MAPK, and concurrent NF-κB inhibition [28]. Similarly, Liu and colleagues reported that in glioblastoma cell lines neither DSF nor copper alone produced measurable cytotoxicity up to 10 μM, whereas their combination lowered the IC_{50} to 120–465 nM through a ROS–JNK/p38 MAPK–NF-κB axis [29]. In colorectal cancer, DSF/copper has also been reported to suppress viability through ULK1-dependent autophagic cell death [11].

The potency shift observed here (approximately 3- to 5-fold) is therefore smaller than the near-complete dependence on added copper described in those studies, in which DSF alone was effectively inactive. This difference is most plausibly attributed to the composition of the basal culture medium. Fetal bovine serum naturally contains small but non-zero amounts of copper, and this trace copper is sufficient to support part of the baseline DSF activity measured in our "no added copper" arm, which was performed in serum-containing medium. Earlier studies probably assessed DSF-alone potency under conditions of more stringent copper restriction. This interpretation is consistent with the failure to reach an IC_{50} in the serum-free DSF arm of the present study and illustrates how sensitive the phenomenon is to the amount of bioavailable copper, even at very low levels. Nevertheless, free copper and intracellular CuET were not measured here, so this explanation remains inferential and should be tested by direct metal and CuET quantification.

The picture of a strict copper dependence, which rests largely on *in vitro* evidence, is not fully mirrored by the available clinical data. In a randomized, placebo-controlled adjuvant trial in high-risk breast cancer, oral sodium diethyldithiocarbamate (dithiocarb), the active metabolite of DSF, was administered without copper supplementation and was associated with markedly better six-year overall survival (81% versus 55% in the placebo arm) [30]. This suggests that *in vivo* the endogenous copper present in serum and tissue may suffice to activate DSF, whereas

most *in vitro* studies, including the present one, add copper to the medium. Colorectal tumor tissue in particular may be copper-rich as a consequence of increased expression of the copper influx transporter CTR1, so that copper available within the tumor microenvironment could be adequate for DSF activation under real conditions [5,36]. Caution is therefore warranted in extrapolating the present *in vitro* doses and, specifically, the apparent requirement for copper supplementation, to a clinical dosing strategy. A further translational caveat comes from the most recent prospective experience with the combination: in a phase 1/2 study of DSF and copper given with radiotherapy and temozolomide in newly diagnosed glioblastoma, CuET was measurable in plasma but could not be detected in tumor tissue, and clinical benefit was confined to a small BRAF-mutant subgroup [14]. Whatever the potency of DSF/copper in cell culture, delivery of the active metabolite to the tumor compartment therefore remains an unresolved obstacle.

4.2 Telomerase activity in intact cells and cell-free lysates

In intact cells, DSF significantly reduced telomerase activity in HCT116 but not in SW480, whereas DSF/copper reduced activity in both lines. One plausible modifier of this difference is p53 status. Using isogenic HCT116 models differing only in p53, Halacli and colleagues showed that telomerase activity and G1 cell-cycle arrest depend on p53 competence, and that in p53 wild-type cells the stress response is accompanied by a decline in telomerase activity [31]. HCT116 carries wild-type p53 whereas SW480 carries mutant p53 [32], so an intact p53 axis may render HCT116 more sensitive to stress-induced telomerase suppression by DSF. In SW480 this pathway is partly disabled, and a significant reduction is achieved only when copper is added and oxidative stress is intensified. However, p53 function was not manipulated here, and the between-line difference therefore cannot be formally assigned to p53 on the basis of these data.

A second notable finding is the reversal of direction in the cell-free system. In contrast to the inhibition seen in intact cells, direct incubation of lysate with copper alone significantly increased telomerase activity by 7.6%, and the DSF–copper combination produced a comparably modest but significant increase of 8.7%. Telomerase, like other polymerases, depends for nucleotide addition on a pair of divalent metal ions held in the active site by three aspartate residues. Lue and colleagues demonstrated that the identity of this metal ion can fundamentally alter catalytic behavior: substituting manganese for magnesium converts telomerase from an RNA-template-dependent enzyme into a template-independent terminal transferase [33]. On this basis, it is plausible that in the simplified lysate environment, which lacks the transcriptional, proteostatic, and redox pressures of a living cell, added copper acts directly on the active site or on the tertiary structure of the telomerase ribonucleoprotein complex and exerts a facilitating or stabilizing effect. This possibility is no longer purely theoretical. Working in fresh colorectal cancer specimens, Shanmugam and colleagues identified the iron sensor Pirin as a factor that reactivates the dormant hTERT subunit of the telomerase holoenzyme in an Fe(III)-dependent manner, and showed that a small molecule competing with iron binding blocks this reactivation [18]. That study provides the first mechanistic demonstration that a metal ion can positively regulate telomerase in this tumor type, and it makes a stimulatory rather than inhibitory response to an added transition metal a biologically plausible outcome rather than an artefact. Because copper binding, enzyme integrity, and amplification efficiency were not measured directly, this modest increase should be treated as an assay-context observation rather than as evidence that copper activates the telomerase active site. Distinguishing a direct active-site effect from a Pirin-like accessory mechanism, and establishing whether copper can substitute for iron in such a role, will require dedicated binding and reconstitution experiments. What the divergence between intact-cell and

lysate responses does establish is that direct catalytic inhibition by DSF is not the mechanism operating under the tested conditions.

Evidence linking dithiocarbamate–copper exposure to telomerase remains limited but is consistent with an indirect route. Abu-Serie and Blasco showed that diethyldithiocarbamate–copper nanocomplexes (DE-Cu_4O_3 and DE-Cu) suppress telomerase activity and reduce nuclear and cytoplasmic TERT as well as TRF1 in non-small-cell lung cancer spheroids, in association with ALDH1A1 inhibition, suppression of p-AKT signaling, and consequent downregulation of TERT expression, together with a fall in mitochondrial membrane potential and mitochondrial DNA copy number [34]. Separately, Deeb and colleagues showed in pancreatic cancer cells that ROS generated by the triterpenoid CDDO-Me suppress hTERT expression and telomerase activity by two concurrent routes: inhibition of AKT phosphorylation, which is required for hTERT activation and nuclear translocation, and suppression of the transcription factors c-Myc, Sp1, and NF-κB that regulate the hTERT promoter. Pretreatment with N-acetylcysteine, or overexpression of SOD1 and glutathione peroxidase, almost completely abolished the effect in that model, establishing a causal role for ROS [21].

Considered together, these observations suggest that the reduction in telomerase activity observed here in intact cells is unlikely to reflect direct catalytic inhibition and is more plausibly a secondary consequence of oxidative stress arising within the living cell. Candidate routes include reduced hTERT transcription mediated by inhibition of AKT, c-Myc, Sp1, and NF-κB, impaired assembly of the telomerase ribonucleoprotein complex, or the complementary ALDH1A1/p-AKT/TERT axis [21,34]. None of these pathways was measured directly in the present study. The interpretation is nevertheless consistent with evidence that hTERT is regulated at both transcriptional and post-translational levels by cellular redox state [21,40,41], and the coupling appears to be bidirectional in the very cell line studied here: in

HCT116 cells, knockdown of TERT or of the telomerase RNA component raises hydrogen peroxide levels and shifts the metabolic profile towards oxidative stress [19]. In the cell-free system these signaling cascades and the transcriptional machinery are absent, so CuET cannot exert its indirect inhibitory effects and only the direct biochemical effect of the copper ion on the enzyme becomes apparent [33].

4.3 Reduced glutathione homeostasis

DSF reduced GSH in both cell lines, copper intensified the decline, and copper alone had no significant effect. The shape of this response is itself informative: an agent that merely consumed glutathione stoichiometrically would be expected to act comparably with and without copper, whereas an agent whose active species forms only in the presence of copper should produce precisely the copper-conditional pattern observed here. This is consistent with the established role of DSF in disrupting glutathione homeostasis. In melanoma cells, DSF markedly increased oxidized glutathione (GSSG) and lowered the GSH/GSSG ratio, an effect attributed principally to inhibition of glutathione reductase (GSR), the enzyme that regenerates GSH from GSSG [16]. Reviews of glutathione in cancer progression and chemoresistance likewise indicate that DSF does not necessarily reduce total glutathione but rather shifts the GSH/GSSG balance towards the oxidized state [35], and DSF has been reported to compete at the GSR active site, disrupting the glutathione regeneration cycle and rendering the cellular redox balance more oxidizing [36].

Because only reduced glutathione was measured in the present study, the decline observed in the DSF-treated groups probably reflects impaired GSH recycling and a fall in the GSH/GSSG ratio, as reported in those studies [15,16,35,36], rather than complete depletion of the total glutathione pool. Concurrent measurement of GSSG will be necessary in future work to resolve this distinction.

The greater fall in GSH in the DSF–copper group relative to DSF alone may be explained by a complementary chemical mechanism operating alongside enzymatic GSR inhibition. This mechanism was not investigated directly here and is proposed on the basis of the published literature. CuET is redox-active and can participate in oxidation–reduction reactions and in transitions between copper oxidation states; for related copper complexes, participation in thiol oxidation with concomitant reduction of Cu(II) to Cu(I) has been demonstrated directly [39]. It is therefore plausible that, in addition to inhibiting GSR, CuET contributes to the oxidation of glutathione thiols. This dual mechanism is consistent with the simultaneous, copper-dependent rise in ROS reported below. Furthermore, DSF itself contains a reactive disulfide bond capable of reacting directly with the sulfhydryl group of GSH to form dithiocarbamate–glutathione adducts or GSSG. The fall in GSH observed here may therefore arise not only from GSR inhibition and consumption of GSH in neutralizing ROS, but in part from direct chemical reaction of DSF with free intracellular thiols. Copper(II) is known to enhance the cytotoxic chemistry of DSF in cancer cells [37], and DSF facilitates intracellular copper accumulation in melanoma cells [38], but direct oxidation of GSH by CuET was not measured here.

4.4 Intracellular reactive oxygen species

DSF increased intracellular ROS in both cell lines, copper further potentiated the increase, and copper alone did not alter baseline ROS. The reciprocity of the GSH and ROS changes, measured in the same cells at the same time point, is worth noting: the two indices moved in opposite directions and to a comparable degree, which is what would be expected if a single copper-dependent oxidative insult were driving both, rather than two independent processes happening to coincide. Two complementary mechanisms may account for this, although neither was examined directly in the present study and both are inferred from the literature. First, by chelating intracellular copper, DSF can withdraw the metal from copper-dependent enzymes, most notably copper/zinc superoxide dismutase (SOD1), thereby reducing the capacity of the

cell to detoxify the superoxide radical [36]. Second, the redox-active CuET complex may participate directly in ROS generation and in the oxidation of thiol groups on mitochondrial proteins, which, if it occurs, would lead to mitochondrial dysfunction [36]. Together these two proposed mechanisms can account for the pro-oxidant effect observed in both cell lines and for its greater magnitude in the DSF–copper group. Copper-dependent DSF cytotoxicity has previously been associated with ROS-sensitive MAPK and NF-κB signaling [28,29] and with redox-active copper–dithiocarbamate chemistry [37,38]. The present data establish the direction and magnitude of the fluorescence response but do not identify the ROS species, the subcellular source, or the contribution of individual antioxidant enzymes.

4.5 Integrated interpretation and proposed mechanistic model

Taken together, the findings support a staged working model. It should be emphasized that several links in this chain, particularly the first step, are drawn from earlier studies and were not measured directly here; the model is therefore a plausible interpretive framework rather than a demonstrated pathway.

In the first step, and on the basis of previous work, DSF chelates copper to form the redox-active CuET complex. It has also been proposed that DSF may act not only as a chelator but as a copper ionophore, facilitating entry of the ion into the cell. Because of its lipophilicity, the resulting complex can cross the plasma membrane and accumulate intracellularly [5,7,38]. Formation of this complex offers the most plausible basis for the potentiation of antiproliferative activity observed here, since addition of a low copper concentration significantly reduced the DSF IC_{50} in both HCT116 and SW480, whereas no measurable cytotoxicity was seen in the serum-free DSF arm.

In the second step, CuET may increase ROS production both by depriving copper-dependent enzymes, particularly SOD1, of their metal cofactor and by participating in cyclic redox

reactions. This part of the model is directly supported by the present data: DSF alone significantly increased ROS in both cell lines, and the concurrent presence of copper markedly intensified that increase. In addition, disruption of NPL4/p97 by CuET can lead to accumulation of ubiquitinated proteins and to severe proteotoxic and endoplasmic-reticulum stress. The resulting disturbance of calcium homeostasis and mitochondrial damage may constitute an upstream source of ROS, providing a mechanistic link between CuET-mediated targeting of proteostasis, an intracellular ROS surge, and subsequent telomerase suppression [7,8,26,27].

In the third step, the increased oxidative burden on the glutathione defense system, together with probable inhibition of GSSG-to-GSH recycling by GSR, lowers the GSH concentration. This was observed here as a simultaneous, copper-dependent decline in GSH [15,16,35,36].

In the fourth step, the resulting oxidative stress, that is, elevated ROS together with reduced GSH, can indirectly suppress telomerase activity in the living cell. This interpretation is consistent with prior evidence on the sensitivity of telomerase activity and hTERT expression to intracellular redox state [40,41]. Conversely, hTERT can itself modify mitochondrial ROS handling and survival responses [40,41], indicating bidirectional coupling rather than a simple one-way pathway. This final link was not tested directly here and must be interpreted with caution.

Copper alone, in the absence of a complete cellular environment and the upstream pathways described, showed no direct inhibitory effect on telomerase. Telomerase inhibition in the intact-cell system is therefore most likely a downstream consequence of a chain of cellular events rather than a direct pharmacological action on the enzyme. The Spearman rank correlations obtained here support this model: GSH correlated with telomerase activity at $\rho = 0.75$, GSH with ROS at $\rho = -0.85$, and ROS with telomerase activity at $\rho = -0.80$, all significant at $P < 0.001$. These coefficients were derived directly from the present data and are consistent with

coordinated changes across treatment conditions. They should not, however, be read as mechanistic proof, particularly because the analysis pooled both cell lines and all treatment groups; correlation alone cannot establish causation. The associations are best regarded as hypothesis-generating evidence that redox state and telomerase response change together, in keeping with reports that treat telomerase not merely as a marker of telomere-length maintenance but as part of the cellular response network to oxidative stress [41].

It is equally important to be clear about what this model does not claim. The redox-telomerase axis described here is one of several processes that DSF and copper are now known to engage in colorectal cancer, and it is almost certainly not the dominant one. Within the same tumor type, the combination drives ULK1-dependent autophagic cell death [11], induces autophagy through both proteasome inhibition and c-Fos-driven BECN1 transcription [12], and remodels the tumor microenvironment so as to increase natural killer and T-cell cytotoxicity [13]. Growth inhibition in the present experiments is therefore best attributed to the established proteotoxic mechanism of CuET rather than to loss of telomerase activity, which over a 24-hour exposure could not plausibly produce a measurable change in telomere length or replicative capacity. What these data add is a different kind of observation: that the redox disturbance accompanying this cytotoxicity is quantitatively coupled to a reproducible fall in telomerase activity, and that this fall is not caused by the drug acting on the enzyme. Whether it represents a functionally consequential arm of the response, an early marker of redox stress, or an epiphenomenon of it, cannot be settled without the interventional experiments outlined below.

5. Limitations

This study has several limitations. First, it was confined to two established colorectal cancer cell lines and lacked non-malignant colorectal controls, so selectivity and generalizability

cannot be established; extension to tumor tissue or animal models will require *in vivo* work. Second, exact passage ranges, STR-authentication dates, and mycoplasma-testing dates were not available in the source records. Third, the relationship among GSH, ROS, and telomerase activity was examined only by correlation analysis; establishing causality requires interventional experiments, such as ROS neutralization with N-acetylcysteine followed by assessment of telomerase recovery. Fourth, no combination-index or isobologram analysis was performed, so formal synergy cannot be claimed. Fifth, hTERT mRNA and protein were not measured, so interpretations concerning transcriptional inhibition or post-translational regulation remain indirect and literature-based. Finally, the study did not measure GSSG, total glutathione, glutathione-reductase activity, intracellular copper or CuET, TERT localization, NPL4 engagement, or pathway-level signaling, and restriction to two colorectal cancer cell lines limits generalizability to other genetic backgrounds, including differing ALDH status and other mutations common in colorectal cancer. These endpoints are needed to distinguish direct from downstream effects.

6. Conclusions and Future Directions

Low, non-cytotoxic concentrations of copper markedly potentiated DSF-induced growth inhibition in HCT116 and SW480 colorectal cancer cells. This response was accompanied by higher ROS, lower GSH, and reduced telomerase activity in intact cells, whereas copper-containing conditions modestly increased telomerase activity in cell-free lysates. The results therefore support an indirect, cellular-context-dependent association between redox imbalance and telomerase suppression, without establishing causality, and they argue against direct inhibition of the telomerase holoenzyme by DSF. The findings support further evaluation of DSF repurposing in combination with copper as a potentially low-cost strategy in colorectal cancer.

Priority next steps are rescue experiments with exogenous antioxidants to test the causal role of ROS in telomerase inhibition; copper-chelation experiments; direct quantification of CuET, GSH/GSSG, and glutathione-reductase activity; measurement of hTERT mRNA and protein together with TERT localization; assessment of NPL4 accumulation and p97/VCP pathway disruption by Western blotting; formal drug-interaction analysis; extension to additional authenticated cancer and non-malignant colorectal models with differing genetic backgrounds, particularly with respect to p53; and validation in xenograft models to evaluate the efficacy and safety of this combination approach *in vivo*. Given that CuET has been detected in plasma but not in tumor tissue in the clinical setting [14], any translational programme built on these findings will also need to address delivery of the active metabolite to the tumor compartment.

Statements and Declarations

Funding

The authors declare that no funds, grants, or other support were received during the preparation of this manuscript.

Competing interests

The authors have no relevant financial or non-financial interests to disclose.

Author contributions

Mohsen Tatar: conceptualization, study design, supervision, and writing—review and editing. Mehdi Khorrami: methodology, investigation, data curation, formal analysis, visualization, and writing—original draft. Jahanbakhsh Asadi: formal analysis, interpretation, and writing—review and editing. All authors read and approved the final manuscript.

Ethics approval

This *in vitro* study used established human colorectal cancer cell lines and involved no human participants, animals, or identifiable human biological material. The study protocol was reviewed and approved by the Ethics Committee of Golestan University of Medical Sciences (approval code IR.GOUMS.REC.1403.113), and institutional biosafety procedures were followed.

Consent to participate

Not applicable.

Consent to publish

Not applicable.

Use of artificial intelligence

During the preparation of this manuscript the authors used an AI-based large language model (Claude, Anthropic) to assist with language editing, readability, and consistency of formatting. The tool was not used to generate, analyse, or interpret experimental data, and it did not contribute to the study design, the scientific content, or the conclusions. All data acquisition, analysis, and interpretation were performed by the authors, who reviewed and edited the resulting text and take full responsibility for the content of the published article.

Declaration of originality

The authors declare that all data presented in this manuscript were generated in-house and that no paper mill was used.

Data availability

The datasets generated and analyzed during the current study are available from the corresponding author on reasonable request.

References

1. Bray F, Laversanne M, Sung H, et al (2024) Global cancer statistics 2022: GLOBOCAN estimates of incidence and mortality worldwide for 36 cancers in 185 countries. CA Cancer J Clin 74, 229-263. https://doi.org/10.3322/caac.21834
2. Zhang J, Ou D, Xie A, Chen D, Li X (2024) Global burden and cross-country health inequalities of early-onset colorectal cancer and its risk factors from 1990 to 2021 and its projection until 2036. BMC Public Health 24, 3124. https://doi.org/10.1186/s12889-024-20624-4
3. Ghasemi-Kebria F, Jafari-Delouie N, Semnani S, et al (2023) Colorectal cancer incidence trends in Golestan, Iran: an age-period-cohort analysis 2004-2018. Cancer Epidemiol 86, 102415. https://doi.org/10.1016/j.canep.2023.102415
4. Pushpakom S, Iorio F, Eyers PA, et al (2019) Drug repurposing: progress, challenges and recommendations. Nat Rev Drug Discov 18, 41-58. https://doi.org/10.1038/nrd.2018.168
5. Kannappan V, Ali M, Small B, et al (2021) Recent advances in repurposing disulfiram and disulfiram derivatives as copper-dependent anticancer agents. Front Mol Biosci 8, 741316. https://doi.org/10.3389/fmolb.2021.741316
6. Chen D, Cui QC, Yang H, Dou QP (2006) Disulfiram, a clinically used anti-alcoholism drug and copper-binding agent, induces apoptotic cell death in breast cancer cultures and xenografts via inhibition of the proteasome activity. Cancer Res 66, 10425-10433. https://doi.org/10.1158/0008-5472.CAN-06-2126
7. Skrott Z, Mistrik M, Andersen KK, et al (2017) Alcohol-abuse drug disulfiram targets cancer via p97 segregase adaptor NPL4. Nature 552, 194-199. https://doi.org/10.1038/nature25016
8. Skrott Z, Majera D, Gursky J, et al (2019) Disulfiram's anti-cancer activity reflects targeting NPL4, not inhibition of aldehyde dehydrogenase. Oncogene 38, 6711-6722. https://doi.org/10.1038/s41388-019-0915-2
9. Tsvetkov P, Coy S, Petrova B, et al (2022) Copper induces cell death by targeting lipoylated TCA cycle proteins. Science 375, 1254-1261. https://doi.org/10.1126/science.abf0529
10. Guo Z, Chen D, Yao L, et al (2025) The molecular mechanism and therapeutic landscape of copper and cuproptosis in cancer. Signal Transduct Target Ther 10, 149. https://doi.org/10.1038/s41392-025-02192-0
11. Hu Y, Qian Y, Wei J, et al (2021) The disulfiram/copper complex induces autophagic cell death in colorectal cancer by targeting ULK1. Front Pharmacol 12, 752825. https://doi.org/10.3389/fphar.2021.752825

12. Wang K, Wang Z, Peng W, et al (2025) Disulfiram activates autophagy via proteasome inhibition and c-Fos/beclin-1 upregulation, synergizing with chloroquine. Cell Death Discov 12, 43. https://doi.org/10.1038/s41420-025-02899-7

13. Dumut DC, Hajduch M, Zacharias AM, et al (2025) Diethyldithiocarbamate-copper complex ignites the tumor microenvironment through NKG2D-NKG2DL axis. Front Immunol 16, 1491450. https://doi.org/10.3389/fimmu.2025.1491450

14. Huang J, Campian JL, DeWees TA, et al (2024) A phase 1/2 study of disulfiram and copper with concurrent radiation therapy and temozolomide for patients with newly diagnosed glioblastoma. Int J Radiat Oncol Biol Phys 120, 738-749. https://doi.org/10.1016/j.ijrobp.2024.05.009

15. Bansal A, Simon MC (2018) Glutathione metabolism in cancer progression and treatment resistance. J Cell Biol 217, 2291-2298. https://doi.org/10.1083/jcb.201804161

16. Cen D, Gonzalez RI, Buckmeier JA, et al (2002) Disulfiram induces apoptosis in human melanoma cells: a redox-related process. Mol Cancer Ther 1, 197-204. PMID: 12467214

17. Kim NW, Piatyszek MA, Prowse KR, et al (1994) Specific association of human telomerase activity with immortal cells and cancer. Science 266, 2011-2015. https://doi.org/10.1126/science.7605428

18. Shanmugam R, Majee P, Shi W, et al (2024) Iron-(Fe3+)-dependent reactivation of telomerase drives colorectal cancers. Cancer Discov 14, 1940-1963. https://doi.org/10.1158/2159-8290.CD-23-1379

19. Samad MA, Saiman MZ, Abdul Majid N, Karsani SA, Yaacob JS (2024) Berberine and RNAi-targeting telomerase reverse transcriptase (TERT) and/or telomerase RNA component (TERC) caused oxidation in colorectal cancer cell line, HCT 116: an integrative approach using molecular and metabolomic studies. Cell Biochem Biophys 82, 153-173. https://doi.org/10.1007/s12013-023-01210-8

20. Borras C, Esteve JM, Vina JR, et al (2004) Glutathione regulates telomerase activity in 3T3 fibroblasts. J Biol Chem 279, 34332-34335. https://doi.org/10.1074/jbc.M402425200

21. Deeb D, Gao X, Liu Y, et al (2013) Inhibition of telomerase activity by oleanane triterpenoid CDDO-Me in pancreatic cancer cells is ROS-dependent. Molecules 18, 3250-3265. https://doi.org/10.3390/molecules18033250

22. Bradford MM (1976) A rapid and sensitive method for the quantitation of microgram quantities of protein utilizing the principle of protein-dye binding. Anal Biochem 72, 248-254. https://doi.org/10.1016/0003-2697(76)90527-3

23. Tatar M, Bagheri Z, Varedi M, Naghibalhossaini F (2019) Blackberry extract inhibits telomerase activity in human colorectal cancer cells. Nutr Cancer 71, 461-471. https://doi.org/10.1080/01635581.2018.1506491

24. Rahman I, Kode A, Biswas SK (2006) Assay for quantitative determination of glutathione and glutathione disulfide levels using enzymatic recycling method. Nat Protoc 1, 3159-3165. https://doi.org/10.1038/nprot.2006.378

25. Wang H, Joseph JA (1999) Quantifying cellular oxidative stress by dichlorofluorescein assay using microplate reader. Free Radic Biol Med 27, 612-616. https://doi.org/10.1016/S0891-5849(99)00107-0

26. Majera D, Skrott Z, Chroma K, et al (2020) Targeting the NPL4 adaptor of p97/VCP segregase by disulfiram as an emerging cancer vulnerability evokes replication stress and DNA damage while silencing the ATR pathway. Cells 9, 469. https://doi.org/10.3390/cells9020469

27. Kanellis DC, Zisi A, Skrott Z, et al (2023) Actionable cancer vulnerability due to translational arrest, p53 aggregation and ribosome biogenesis stress evoked by the disulfiram metabolite CuET. Cell Death Differ 30, 1666-1678. https://doi.org/10.1038/s41418-023-01167-4

28. Yip NC, Fombon IS, Liu P, et al (2011) Disulfiram modulated ROS-MAPK and NFkappaB pathways and targeted breast cancer cells with cancer stem cell-like properties. Br J Cancer 104, 1564-1574. https://doi.org/10.1038/bjc.2011.126

29. Liu P, Brown S, Goktug T, et al (2012) Cytotoxic effect of disulfiram/copper on human glioblastoma cell lines and ALDH-positive cancer-stem-like cells. Br J Cancer 107, 1488-1497. https://doi.org/10.1038/bjc.2012.442

30. Dufour P, Lang JM, Giron C, et al (1993) Sodium dithiocarb as adjuvant immunotherapy for high risk breast cancer: a randomized study. Biotherapy 6, 9-12. https://doi.org/10.1007/BF01877380

31. Halacli SO, Canpinar H, Cimen E, Sunguroglu A (2013) Effects of gamma irradiation on cell cycle, apoptosis and telomerase activity in p53 wild-type and deficient HCT116 colon cancer cell lines. Oncol Lett 6, 807-810. https://doi.org/10.3892/ol.2013.1441

32. Zhang Y, Devocelle A, Souza L, et al (2020) BMAL1 knockdown triggers different colon carcinoma cell fates by altering the delicate equilibrium between AKT/mTOR and P53/P21 pathways. Aging (Albany NY) 12, 8067-8083. https://doi.org/10.18632/aging.103124

33. Lue NF, Bosoy D, Moriarty TJ, et al (2005) Telomerase can act as a template- and RNA-independent terminal transferase. Proc Natl Acad Sci USA 102, 9778-9783. https://doi.org/10.1073/pnas.0502252102

34. Abu-Serie MM, Blasco MA (2025) Diethyldithiocarbamate-Cu4O3 nanocomplex induced mitochondrial and telomerase dysfunction in non-small-cell lung cancer. Nanomedicine (Lond) 20, 1267-1280. https://doi.org/10.1080/17435889.2025.2502321

35. Traverso N, Ricciarelli R, Nitti M, et al (2013) Role of glutathione in cancer progression and chemoresistance. Oxid Med Cell Longev 2013, 972913. https://doi.org/10.1155/2013/972913

36. Meraz-Torres F, Ploger S, Garbe C, Niessner H, Sinnberg T (2020) Disulfiram as a therapeutic agent for metastatic malignant melanoma - old myth or new logos? Cancers 12, 3538. https://doi.org/10.3390/cancers12123538

37. Tawari PE, Wang Z, Najlah M, et al (2015) The cytotoxic mechanisms of disulfiram and copper(II) in cancer cells. Toxicol Res 4, 1439-1442. https://doi.org/10.1039/C5TX00210A

38. Cen D, Brayton D, Shahandeh B, Meyskens FL Jr, Farmer PJ (2004) Disulfiram facilitates intracellular Cu uptake and induces apoptosis in human melanoma cells. J Med Chem 47, 6914-6920. https://doi.org/10.1021/jm049568z

826 39. Ramirez-Palma LG, Espinoza-Guillen A, Nieto-Camacho F, et al (2021) Intermediate detection
827 in the Casiopeina-cysteine interaction ending in the disulfide bond formation and copper
828 reduction. Molecules 26, 5729. https://doi.org/10.3390/molecules26195729

829 40. Indran IR, Hande MP, Pervaiz S (2011) hTERT overexpression alleviates intracellular ROS
830 production, improves mitochondrial function, and inhibits ROS-mediated apoptosis in cancer
831 cells. Cancer Res 71, 266-276. https://doi.org/10.1158/0008-5472.CAN-10-1588

832 41. Green PD, Sharma NK, Santos JH (2019) Telomerase impinges on the cellular response to
833 oxidative stress through mitochondrial ROS-mediated regulation of autophagy. Int J Mol Sci
834 20, 1509. https://doi.org/10.3390/ijms20061509

835 # Tables

836 Table 1 Primer sequences used in the telomeric repeat amplification protocol (TRAP) assay and its internal
837 control

Primer category	Primer	Sequence (5′→3′)	Function
Telomerase assay	TS (substrate)	AATCCGTCGAGCAGAGTT	Substrate primer extended by telomerase
Telomerase assay	ACX (reverse)	GCGCGG[CTTACC]$_3$CTAACC	Reverse primer for PCR amplification of telomerase products
Internal control	NT	ATCGCTTCTCGGCCTTTT	Amplifies the internal control fragment
Internal control	TSNT	AATCCGTCGAGCAGAGTTAAAAGGCCGAGAAGCGAT	Template generating the 36-bp internal control band, excluding false negatives

838 Primers were custom-synthesized (Pishgam Biotech, Tehran, Iran). The subscript 3 in the ACX sequence denotes three
839 tandem repeats of the bracketed hexamer.

840 Table 2 Growth-inhibitory effect of disulfiram and copper on the human colorectal cancer cell lines HCT116
841 and SW480 after 48 h of treatment (calculated IC_{50} values)

Cell line	Treatment group	IC_{50} (µM)	Potentiation by copper
HCT116	Disulfiram + serum	2.04	—
HCT116	Disulfiram + serum + 0.1 µM Cu	0.39	≈ 5.3-fold
HCT116	Copper + serum	Not calculable (> 20)	—
HCT116	Disulfiram, serum-free	Not calculable (> 20)	—
SW480	Disulfiram + serum	1.73	—
SW480	Disulfiram + serum + 0.1 µM Cu	0.56	≈ 3.1-fold
SW480	Copper + serum	Not calculable (> 20)	—

Cell line	Treatment group	IC_{50} (μM)	Potentiation by copper
SW480	Disulfiram, serum-free	Not calculable (> 20)	—

IC_{50} values were derived from the dose–response curves in Figs. 1 and 2 using GraphPad Prism. Copper was used at a fixed sub-toxic concentration of 0.1 μM (100 nM).

Table 3 Telomerase activity, reduced glutathione, and intracellular reactive oxygen species in HCT116 and SW480 cells after 24 h of treatment

Cell line	Treatment	Telomerase activity (%)	GSH (μM/mg protein)	ROS (RFU)
HCT116	Control	101.5 ± 2.25	22.30 ± 0.60	116.6 ± 5.2
HCT116	Cu (0.1 μM)	98.4 ± 1.56	21.40 ± 0.70	121.3 ± 6.0
HCT116	DSF (0.5 μM)	86.8 ± 4.26**	18.86 ± 1.64*	158.3 ± 10.4***
HCT116	DSF + Cu	69.4 ± 8.22***	14.94 ± 1.27***	193.1 ± 17.8***
SW480	Control	100.9 ± 2.55	24.60 ± 1.00	102.2 ± 6.8
SW480	Cu (0.1 μM)	99.5 ± 3.50	23.90 ± 0.90	105.0 ± 2.9
SW480	DSF (0.5 μM)	95.0 ± 5.39 ns	22.64 ± 1.78*	135.4 ± 5.1***
SW480	DSF + Cu	78.6 ± 6.97***	18.75 ± 1.27*	156.4 ± 9.1***

Values are mean ± SD of six independent biological replicates per group, each read in technical duplicate. Comparisons are versus the vehicle-matched control of the same cell line (one-way ANOVA with Tukey's multiple-comparison test). *P < 0.05; **P < 0.005; ***P < 0.001; ns, not significant. DSF, disulfiram; Cu, copper sulfate; GSH, reduced glutathione; ROS, reactive oxygen species; RFU, relative fluorescence units.

Table 4 Spearman rank correlation among reduced glutathione (GSH), reactive oxygen species (ROS), and telomerase activity

Index pair	Spearman ρ	P value	Relationship
GSH ↔ Telomerase activity	0.75	< 0.001	Strong positive
GSH ↔ ROS	−0.85	< 0.001	Strong negative
ROS ↔ Telomerase activity	−0.80	< 0.001	Strong negative

Analysis was performed on 48 values per index (two cell lines × four treatment groups × six independent biological replicates). The non-parametric Spearman test was used because the pooled data for each index departed from normality on the Shapiro–Wilk test.

Figures

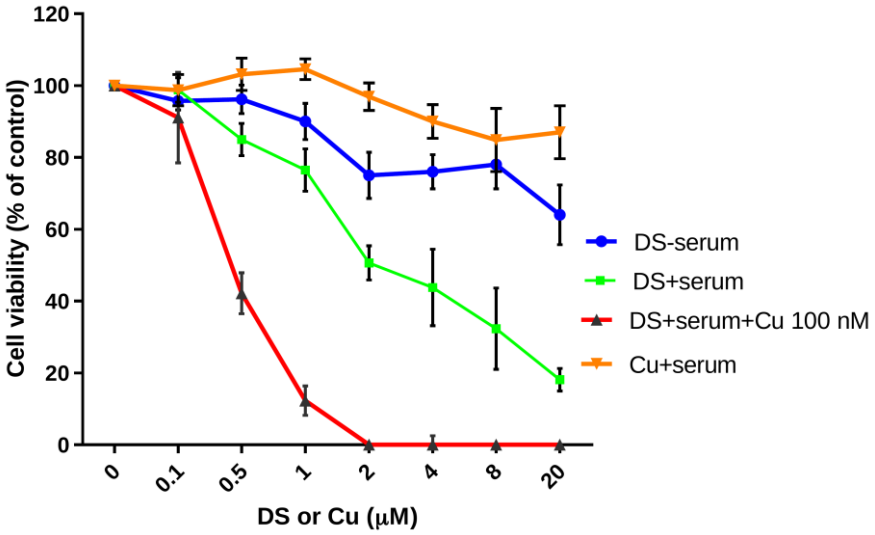


Fig. 1 Sensitivity of the HCT116 colorectal cancer cell line to growth inhibition by disulfiram and copper. Cells were exposed for 48 h to increasing concentrations of disulfiram and copper, alone or in combination, and proliferation was determined by MTT assay as described in Materials and Methods. Cell viability is shown relative to the untreated control. DS, disulfiram. Data are mean ± SD of six independent experiments.

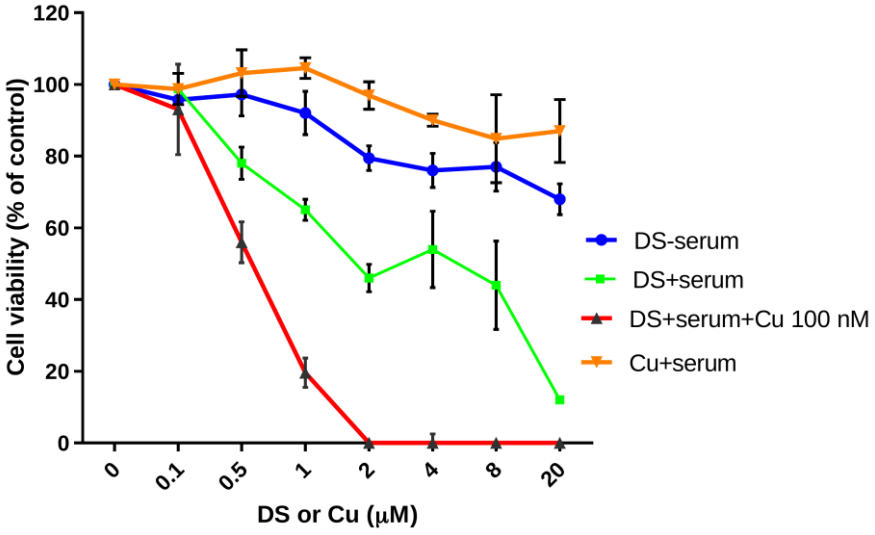


Fig. 2 Sensitivity of the SW480 colorectal cancer cell line to growth inhibition by disulfiram and copper. Conditions and analysis were identical to those in Fig. 1. Cell viability is shown relative to the untreated control. DS, disulfiram. Data are mean ± SD of six independent experiments.

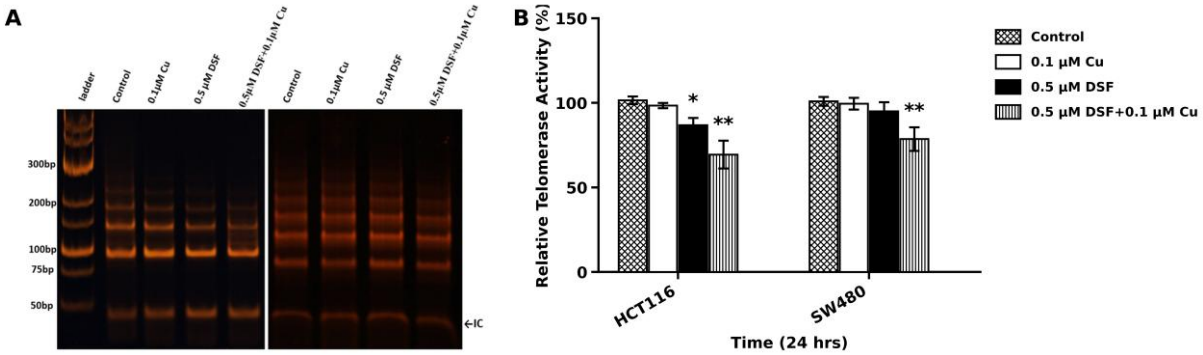


Fig. 3 Effect of disulfiram and copper on telomerase activity in intact HCT116 and SW480 colorectal cancer cells. (A) Representative TRAP gels after 24 h of treatment; left gel, HCT116; right gel, SW480. Lanes (left to right): DNA ladder (left gel only), untreated control, 0.1 μM Cu, 0.5 μM DSF, and 0.5 μM DSF + 0.1 μM Cu. A reduction in the number and intensity of telomeric ladder bands indicates lower telomerase activity. IC, 36-bp internal amplification control (arrow). (B) Densitometric quantification of relative telomerase activity, calculated from telomeric ladder intensity and normalized to the untreated control (100%). Data are mean ± SD of six independent experiments. *P* values were calculated by one-way ANOVA with Tukey's multiple-comparison test; **P* < 0.005 and ***P* < 0.001 versus the untreated control.

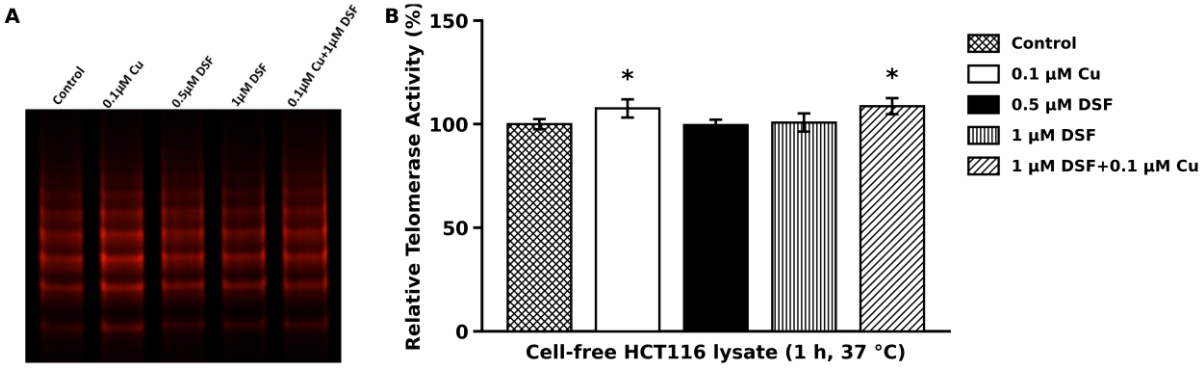
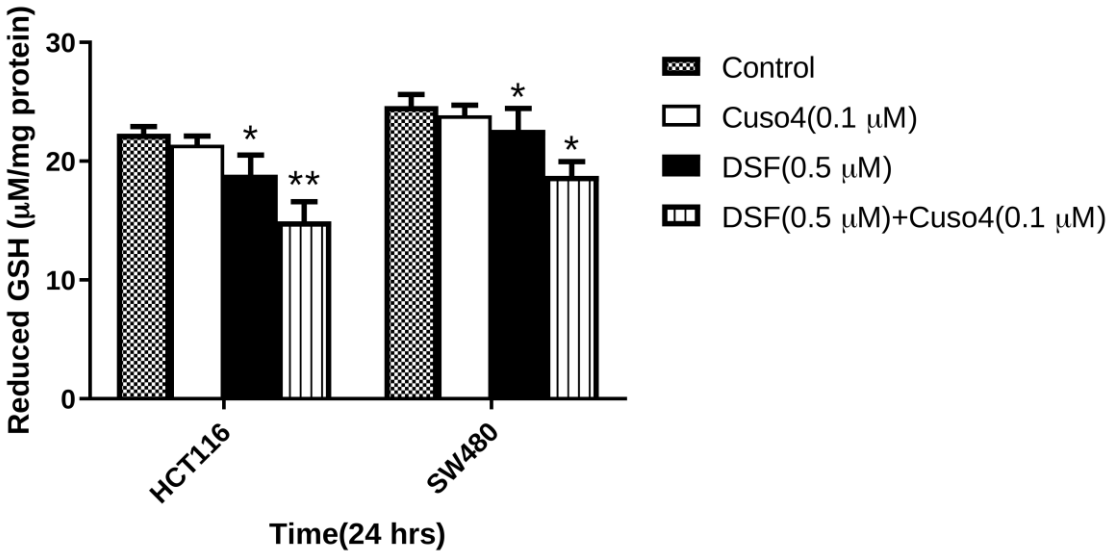
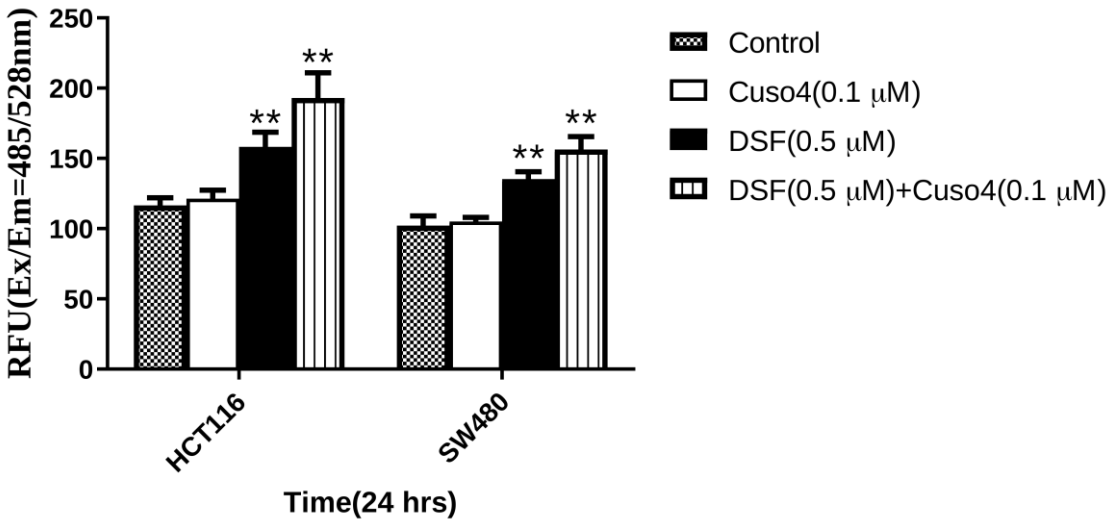


Fig. 4 Effect of disulfiram and copper on telomerase activity in a cell-free system. (A) Representative TRAP gel of cell-free HCT116 lysate. Lanes (left to right): untreated control, 0.1 μM Cu, 0.5 μM DSF, 1 μM DSF, and 0.1 μM Cu + 1 μM DSF. Lysate (2 μg protein) was incubated with each condition for 1 h at 37 °C before TRAP analysis; telomeric ladders were retained in all lanes. (B) Densitometric quantification of relative telomerase activity normalized to the untreated control (100%). Data are mean ± SD of three independent experiments. **P* < 0.05 versus the untreated control (one-way ANOVA with Tukey's multiple-comparison test).



881

882 Fig. 5 Effect of disulfiram and copper on the concentration of reduced glutathione (GSH) in HCT116 and SW480
883 colorectal cancer cells. Cells were treated for 24 h, and GSH in the cell lysate was measured and expressed as μM
884 per mg total protein. Data are mean ± SD of six independent experiments. *P* values were calculated by one-way
885 ANOVA with Tukey's multiple-comparison test; **P* < 0.05 and ***P* < 0.001 versus the untreated control.



886

887 Fig. 6 Effect of disulfiram and copper on the level of intracellular reactive oxygen species (ROS) in HCT116 and
888 SW480 colorectal cancer cells. Cells were treated for 24 h, and intracellular ROS were measured fluorometrically
889 and expressed as relative fluorescence units (RFU) at excitation/emission wavelengths of 485/528 nm. Data are
890 mean ± SD of six independent experiments. ***P* < 0.001 versus the untreated control (one-way ANOVA with
891 Tukey's multiple-comparison test).